Controlling the Synthesis of Branched Gold Nanoparticles using a Wet Chemical Synthesis Method

Master's Final Year Project Report

Hugo Day
School of Physics and Astronomy
University of Southampton
University Road
Southampton
Hampshire
SO17 3SX

30th April 2009

Controlling the Synthesis of Branched Gold Nanoparticles using a Wet Chemical Synthesis Method

Abstract

A wet chemical synthesis method was successfully used to produce branched gold nanoparticles. It was found that by varying the initial conditions of the reaction it is possible to exert control on the strtuctural characteristics of the resulting nanoparticles. Optical measurements revealed that changes in the physical structure resulted in red-shifting of the absoprtion peak of the nanoparticles, contributed to by the changing plasmon resonance peaks of the nanoparticles.

1 Contents

2 Introduction

Nanoscience has provided a plethora of novel systems, applications and scientific research within the last twenty years, but has a history extending back over 100 years. Although Faraday produced colloidal gold nanoparticles in the 19th century[1], it was not until the late 1980s and early 1990s that large breakthroughs began to be made. It has been found that metallic nanoparticles have unique optical and physical properties, which derive from the difference in between the properties of bulk materials and small (on the order of nanometres) clusters of atoms.

The initial production of anisotropic nanoaparticles was using semiconducting materials (e.g. cadmium selenide, cadmium teluride etc.). This has led to the production of the structures known as quantum dots; essentially quantum wells restricted in all 3 spatial dimensions in which the allowed energy states can be controlled by varying the dimensions of the quantum dot. This allows the selective choosing of the absorption/emission of light by photon energy. This holds promise for use in photovoltaic cells to increase the efficiency of energy conversion[2], quantum computation [3] and to some extent in biological applications[4], although the toxicity of the materials used remains a significant issue in this area[5].

The second expansion in this area of research has been the progressive discovery of the techniques required to make anisotropic structures from noble metallic structures which typically have a face centred cubic (fcc) lattice structure and so do not typically grow anisotropic structures as they are not thermodynamically favourable. This has been achieved largely by experimental methods, with the theoretical background to the mechanisms coming after detailed investigation of the experimental procedures and conditions[6].

This has led to the ability to produce rod-like structures of various kinds, cubes, bipyramids, and more recently branched nanoparticles. These changes in the structure cause changes in both the optical properties and the structural properties of the particles, despite being composed of the same element. The changes in physical properties originate from the detailed surface chemistry that the particles experience, whilst the changes in optical properties have their basis in a phenomenon known as localised surface plasmon resonance (LSPR) (explained in section 2.1). These unique properties provide a plethora of potential applications; intense research currently occurs in biomedical applications for imaging methods and the potential for localised treatment by the coating of nanoparticles in receptor specific biological markers[7], the use of particles as a template

for polymer growth[8] and to increase the efficiency of catalytic methods of production[9].

An example of the intended applications of these molecules is their use to increase the surface-enhanced Raman scattering (SERS) activity. It has been shown in recent research that branched gold nanoparticles can cause the emission of SERS signals up to 10 times greater than the equivalent signal generated with gold nanospheres coated in the same biological marker.[15]. This is again due to the localised surface plasmon resonance that occurs at the tips of branches and in the crevices of the particles causing very large local electric fields and thus causing great SERS intensity.

Their low level of toxicity is seen as a primary advantange, as semi-conductor nanoparticles are too toxic to be considered for biological usage, whereas noble metal nanoparticles are largely inert in biological systems.

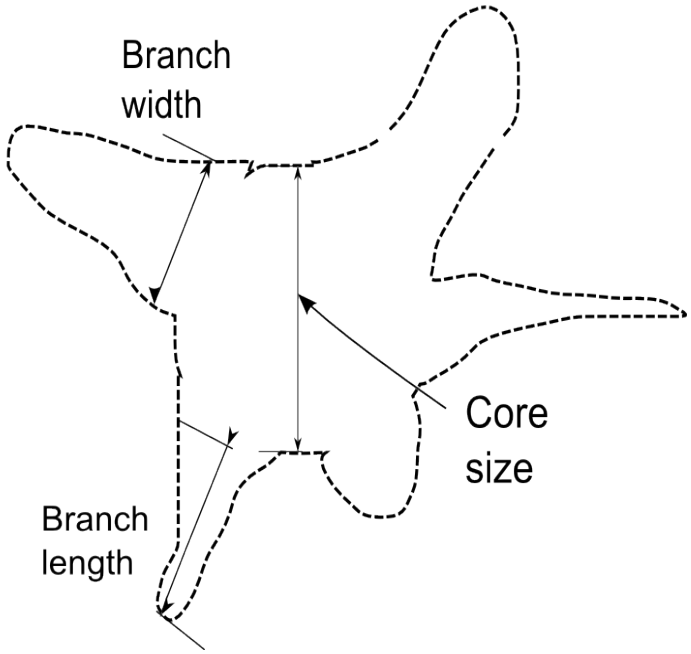

Figure 1: *A 2-dimensional illustration of a typical branched nanoparticle with its physical characteristics labelled.*

Current research in the area of branched nanoparticles primarily focuses on their applications with additional research into the complex mechanisms behind the growth also becoming more intensely investigated as more applications for this family of particles are studied. To this end, this project will investigate the limits to which the physical and optical characteristics of branched nanoparticles can be controlled by altering the initial conditions of a wet chemical synthesis method.

2.1 Localised Surface Plasmon Resonance

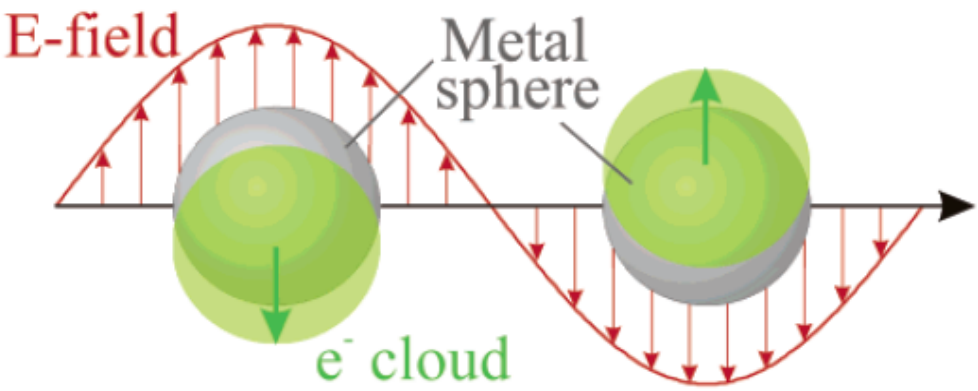

Figure 2: *The oscillation of the electron cloud of a metallic nanosphere due to an incident electric field. Use courtesy of Kelly, K.L.; Coronado, E.; Zhao, L.L.; Schatz, G.C., 'The Optical Properties of Metal Nanoparticles: The Influence of Size, Shape, and Dielectric Environment', J. Phys. Chem. B 2003, 107, 668-677*

Surface plasmon resonance is the bulk oscillation of electrons at the boundary of two mediums. In this experiment, the particles used used are gold and water. These can be considered localised when the surface they exist on is exceptionally small, as is the case for nanoparticles, and as is illustrated in fig 2. It is possible to determine the extinction cross section of incident light on the particle by solving Maxwell's equations for a particle composed of a substance with a complex wavelength dependent dielectric function ε_i, surrounded by a medium with a dielectric constant ε_m, which derives[10] to

$$Q_{ext} = \frac{8\pi a \varepsilon_0^{\frac{1}{2}} \Im(g_d)}{\lambda} \qquad (1)$$

where a is the radius of the particle, λ is the wavelength of the incident light and:

$$g_d = \frac{\varepsilon_i - \varepsilon_0}{\varepsilon_i + 2\varepsilon_0} \qquad (2)$$

This leads to a maximum absorption peak occurring in at a given wavelength, which for the case of a 20nm spherical gold nanoparticle occurs at 520nm[10]. This was first calculated by Gustav Mie in 1908, decades before this became used in nanotechnology[11].

Increasing the size of the particles or changes from the spherical geometry cause the absorption peak to red-shift from this value. For nanorods this is the creation of two absorption peaks; one for the long axis and one for the short axis, similar to as would be expected for a spheroid shape. For branched nanoparticles a variety of peaks can arise due to the complex geometrical shapes that they can form. Oscillation modes may occur between two branches, a branch and the core, across a branch or in a number of different planes across the particle. Also, branched nanoparticles do not typically exhibit the same monodisperse nature of nanorods or nanospheres[10]. However there are typical peaks which occur predominantly throughout a sample which can be utilised. It is the changes of these peaks due to differing geometries, the creation of which can be controlled by the initial conditions of the manufacturing technique which we wish to utilise.

It should be noted that analytical solutions to these systems are only solvable for spherical and ellipsoid shapes, and as such numerical methods have to be used to form solutions for most isotropic shapes. The most commonly used methods are the discrete-dipole-approximation (DDA) and finite difference time-domain (FDTD) techniques to solve Maxwell's equations. DDA methods involve treating particles as a mesh of independently polarisable dipoles and calculating the resulting interactions with an incident electric field[12], whilst the FDTD techniques rely on the repeated solving of Maxwell's equations in a time-evolving spectral grid[10].

3 Mechanism of Reactions

The seeded growth method used in this investigation separates the growth of branched nanoparticles into two stages; the growth of seeds using a strong reducing agent, and the growth of crystal structures from these seeds using a surfactant guided process taking place under a weak reducing agent. Both of these reactions are driven by thermodynamic and kinetic pressures to reduce the free energy available to the system (in this case the molecules and ions in a solution).

3.1 Citrate reduction of $NaAuCl_4$ (aq)

Chemically, this reaction involves the reduction of Au^{3+} ions to Au^0 atoms by citrate ions, which subsequently aggregate to form first small clusters of gold atoms, then congregate into larger clusters (referred to as nuclei), and then grow further to form nanospheres. These two stages are distinguished by the growth of the structure of nuclei being controlled by those structures that have the densest packing of atoms being thermodynamically favourable. Conversely, the growth of seeds is guided by reducing the interfacial free energy of seeds. The progression through these stages is as such:

1. Au^{3+} ions are reduced to Au^0 atoms which form cluster like complexes in suspension

2. Au^0 complexes reach a critical saturation where they begin to form nuclei

3. Nuclei become of size where reducing the interfacial free energy becomes the dominant pressure in determining the structure of the particle.[13]

This distinction is important because once the seed growth phase begins the nuclei are fixed in structure, having either a single crystal structure, single or multi-twinned structure or containing stacking faults. These affect the final shape of the seeds that maybe produced, and consequently what nanostructures will be formed in the crystal growth phase (the effect of the crystal structure on the development of seeds and nanocrystals is shown in figure 4).

The seed growth stage aims to produce particles with a minimum interfacial free energy, as predicted by Wulff's Theroem[14]. If this energy is represented by a factor γ, it can be defined as the energy required to create a unit area of new surface given in eqn. 3

$$\gamma = \left(\frac{\partial G}{\partial A}\right)_{n,T,P} \qquad (3)$$

where G is the free energy of the system, A the surface area and n,T,P are no. of atoms, temperature and pressure of the system respectively. For seeds, the crystal symmetry is broken by missing (or broken) bonds on the surface of the seed, which causes surface atoms to attracted to the particle interior. A restoring force is required to counter this force to move them back to the surface. This

can be simply represented as in eqn. 4

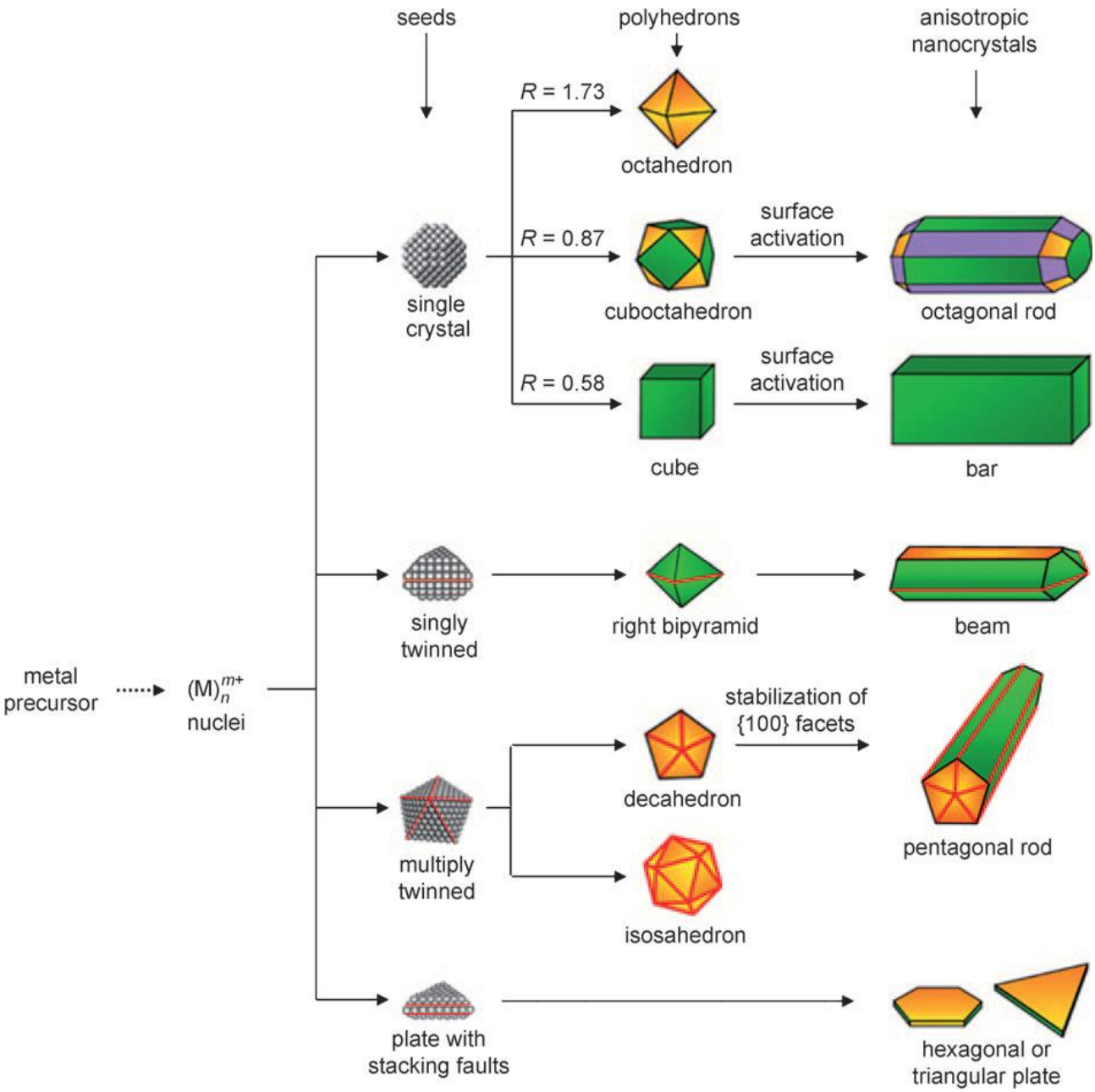

Figure 3: *The different nanocrystalline structures that can be formed from various starting nuclei and seed structures. Green, orange and purple colours represent the [100],[111] and [110] facets respectively. Twin planes a delineated by red lines. The reaction mechanism in this experiment predominantly uses single crystal seeds, with a small proportion of plates with stacking faults, as shown by the presence of hexagons in the final product.*

Image used courtesy of Xia, Y.; Xiong, Y.; Lim,B.; Skrabalak, S.E., 'Shape-controlled synthesis of metal nanocrystals: Simple Chemistry meets Complex Physics?'

$$\gamma = 1/2\, N_b \varepsilon \rho_a \qquad (4)$$

where N_b is the number of broken bonds, ε is the strength of the bond and ρ_a is the density of the surface atoms[13]. The value of γ can subsequently be found to vary depending on the lattice facet that encloses the surface, such that $\gamma_{[111]} < \gamma_{[100]} < \gamma_{[110]}$, where [111],[100],[110] represent lattice vectors in an face centred cubic crystalline structure, which gold forms. Thus it can be seen that [111] and [100] facets should be the predominant facets present on the structure. Structures presenting only the [111] facet do not generally form due to their larger surface area than equal volume structures mixing [111] and [100] facet presentation[13]. Figure 3 shows the possible seeds and the subsequent shapes that can form due to different nuclei structures. The variety of these structures will lead to different populations of branched particles forming, and predicts that there maybe some hexagonal plates and octahedrons within the final product.

When the seed or particle growth stage has ended, the citrate ions subsequently act as ligands on the surface of the seeds to stabilise them.

3.2 Surfactant guided growth of branched nanoparticles

The mechanism that guides the growth of branched nanoparticles from the previously produced seeds is a surfactant guided growth mechanism. This involves the binding of a surfactant molecule to a certain lattice facets to prevent growth along these planes, and thus create anisotropic growth of the particle. The principle of this method is shown in figure 4

In this investigation, we have used the surfactant centrylammonium bromide (CTAB) to guide the growth, along with using Ag^+ as a binding aid. The addition of a source of Ag^+ ions to this solution allows further control, as the surfactant CTAB will preferentially bind to Ag^+ ions due to the bromine atom contained within the molecule. The Ag^+ ions are known to preferentially bind to the highest energy facets available[17], in the case of the seeds used in this experiment this will be the [100] facets. This subsequently causes a layer of surfactant to be present on the [100] facet so that growth of the particle may only occur in the direction of the [111] facet, causing the branched structure to grow.

The structures do not continue to grow indefinitely as the CTAB ligand only binds preferentially to the Ag^+ ions deposited on [100] facets, not exclusively. The [111] facets are bound to also, and thus growth cannot continue. This has been previously observed in the growth of other anisotropic nanocrystalline structures due to the presence of Au^+ being found in the unreacted solution after particles have been recovered and observed to not develop further[16].

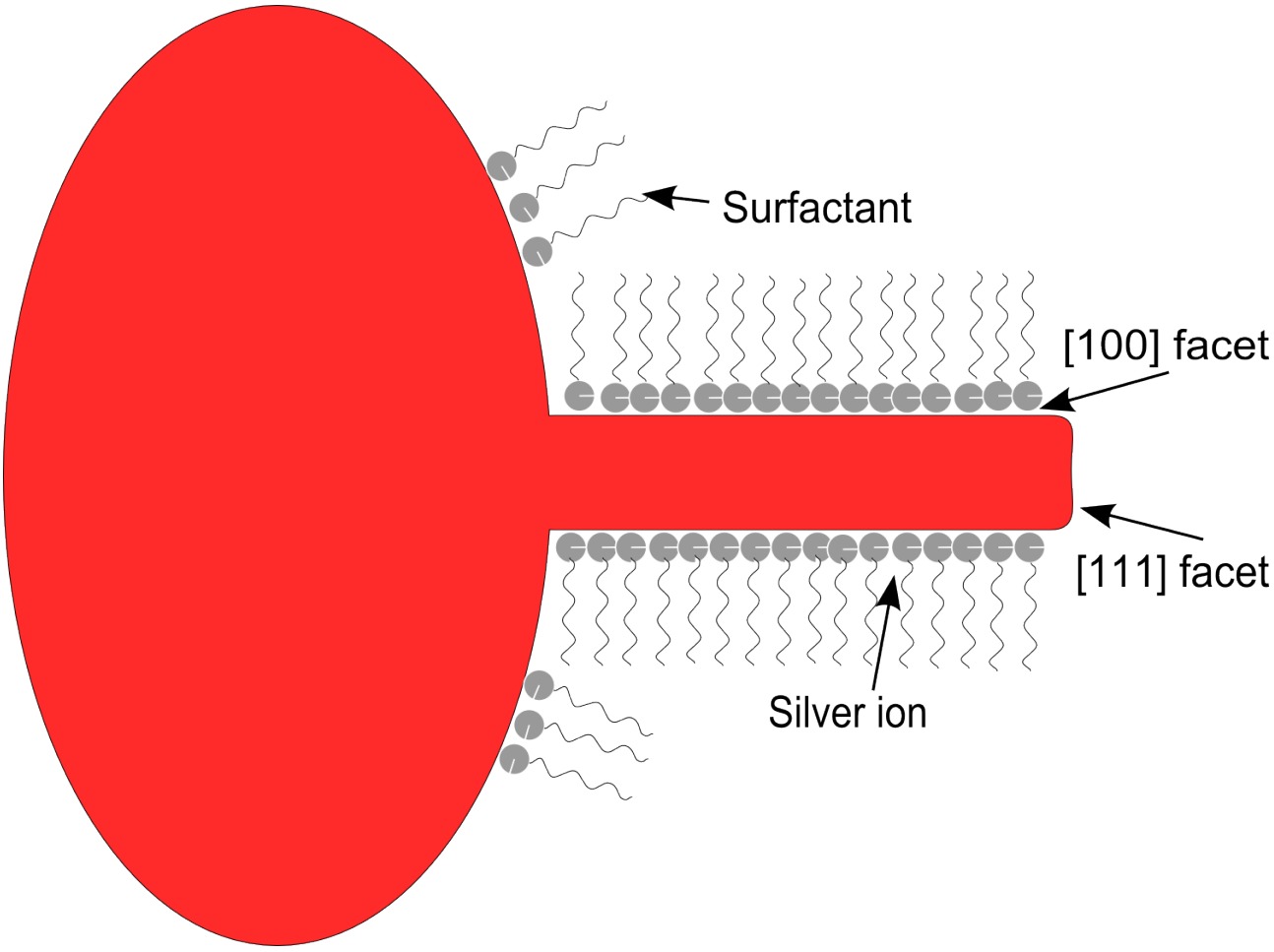

Figure 4: *The surfactant guided growth mechanism of branches from a spherical seed. Growth occurs in the [111] direction due to the preferential binding of CTAB to Ag^+ on the [100] facet.*

4 Experimental Method

4.1 Materials and Metrological Equipment

All reagents were purchased from the following suppliers and were not further altered before use: sodium tetrachloroaurate (III) dihydrate, trisodium citrate, silver nitrate, L-ascorbic acid were purchased from Sigma-Aldrich, bis(p-sulfonatophenyl)phenyl phosphene dehydrate dipotassium salt (BSBP) was purchased from Strem-Chemicals, Inc., hexadecyltrimethylammonium bromide (CTAB) was purchased from Alfa Aesar. Ultra pure millipore water was used as a solvent.

TEM images were obtained with Hitachi H7000 transmission electron microscope operating at a bias voltage of 73.2 kV. All samples were deposited on Carbon Film 400 Mesh Copper (50) grids. UV-Visible spectra were collected using UV-1601 Shimadzu UV-Visible spectrophotometer over the range from 200 to 1000 nm, and Jasco UV/VIS/NIR spectrophotometer.

4.2 Production of BSBP-Coated Gold Nanospheres

Sodium citrate coated gold nanospheres were produced by the citrate reduction of $NaAuCl_4$(aq). The mechanism for this reaction is discussed in 3.1. 25ml of 0.5mM $NaAuCl_4$ salt solution and 2.5ml of 19.5mM sodium citrate solution were added to separate containers and heated to their boiling point. The containers were covered to prevent loss of volume during heating. The sodium citrate solution was then rapidly added to the $NaAuCl_4$ solution under vigorous stirring. This caused a colour change from colourless to dark red/brown.

The mixed $NaAuCl_4$ and sodium citrate solution was allowed to cool to room temperature whilst still under vigorous stirring. The solution was observed to change from dark red/brown to a red. 2.5mg of BSBP was added to the solution, which was left under constant stirring for at least 2 hours. Sufficient sodium chloride to cause a change of colour from red to dark purple was then added. The sample was subsequently centrifuged at 8000RPM and the supernatant then resuspended in water. The solution of BSBP-coated nanospheres was subsequently stored at $<5^{o}C$ in a sealed container.

4.3 Production of Branched Gold Nanoparticles

Branched gold nanoparticles were produced by surfactant guided, seeded, reduction growth method, as discussed in 3.1. A growth solution of 3.56ml 0.2M CTAB solution, 102.5µl 5mM $AgNO_3$ solution and 500µl of 5mM of $NaAuCl_4$ solution was made for each experiment. To this solution, 4µl of the phosphene-coated gold nanospheres were added. 40µl of 0.0788M l-ascorbic acid was added to this solution to commence the reaction. The solution was left for 1.5 to 2 hours. The solution was kept at a temperature between 20-30^{o}C throughout the reaction.

The solution was then placed in a centrifuge at a speed of 8000RPM for 10minutes. The excess solution was removed, and the supernatant resuspended in water and the process repeated again. The particles were suspended in 1ml of water and stored at <5^{o}C in a sealed container.

5 Results and Discussion

Initial experiments to determine the mechanism of the reaction implied that the two reactants which had the most effect on the shape of the produced branched nanoparticles were the concentration of silver nitrate in the growth solution and the concentration of the ascorbic acid used as a reducing agent in the reaction. As such, the experiments were planned to isolate these reactants, and investigate their significance in the reaction mechanism.

5.1 The Effect of Altering the Concentration of Silver Nitrate on the Characteristics of Branched Nanoparticles

The role that silver plays in the mechanism of the growth of the branched nanoparticles is as a preferential binding site for CTAB molecules. This indicates a possibility that, depending on the relative growth rates of the core of the branched nanoparticles and of the arms, raising or reducing the concentration of silver nitrate in the growth solution may change the length of the arms relative to the size of the core. This is an especially useful goal as the optical properties of branched nanoparticles change extensively depending on the length of the arms. Experiments were carried out using the method described in 4.3 but with the following modifications; the concentration of silver was altered between experiments to cover the following concentrations of silver nitrate solution: 2.5mM, 5mM, 10mM, 15mM, 20mM, 25mM, 30mM, 35mM, 40mM, 45mM.

5.1.1 Modification of Physical Properties

The physical changes in the structure of the branched particles produced due to changes in only the concentration of silver nitrate confirm the mechanism of Ag^+ ions acting as preferential binding site for CTAB ligands. This can be seen by the increasingly small size and the increasing proportion of spherical particles in the populations of particles formed, shown in figure 5. This also confirms preferential binding of Ag^+ ions to specific lattice planes of gold which can be inferred due to the thermodynamically driven growth of the particles at very low concentrations of Ag^+ ions, caused due to there not being sufficient silver to cause sufficient surfactant to bind to any lattice plane in preference over another. This is shown by the formation of large populations of bypiramidal and hexagonal structures at a concentration of 6.04 x 10^{-4}M. For non-surfactant guided growth, these are often the shapes thermodynamically preferred by gold crystals as they maximise the surface profile of the [111] lattice vector (see section 3.2 for more details).

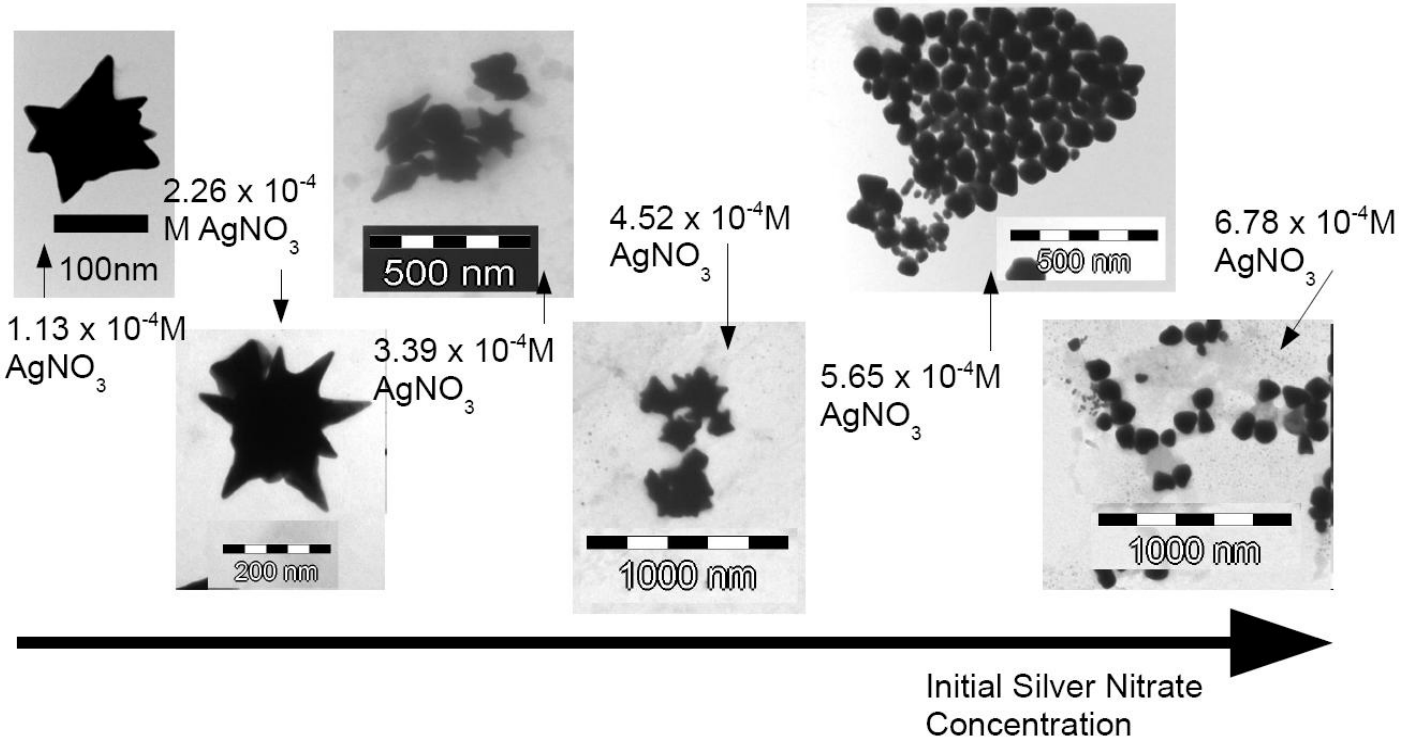

Figure 5: *A display of typical particles produced as a function of the increasing concentration of silver nitrate in the initial reactants. Note the progress towards small spherical particles as the growth phase of the reaction decreases in length*

At higher concentrations, this is achieved in sufficient enough scale to cause anisotropic growth. At very high concentrations of Ag^+ ions, there is sufficient quantity such that all lattice vectors are

bound to in substantial quantity even considering the preferential binding of silver to certain lattice vectors, thus causing minor/no growth to be observed. Note that at high concentrations the produced particles are of the same size of the initial seeds. This indicates that either the particle growth is either very short lived, or does not occur.

5.1.2 Modification of Optical Properties

The effect of increasing the concentration of silver nitrate in the reaction is as would be expected from section 2.1. As figure 7 shows, the peak absorption maximum wavelength decreases steadily with the increase in concentration as the particles produced become less branched until they have similar absorption spectra to spherical nanoparticles with a peak near 550nm for a concentration of 9.04 x 10^{-4}M Ag^{+} ions.

The broad absorption peak seen in the spectrum of the sample corresponding to concentration 6.04 x 10^{-4}M of Ag^{+} ions is to be expected due to the mixed population of the particles it produced, with absorption from spheres, hexagons and the long and short axes of the bipyramids.

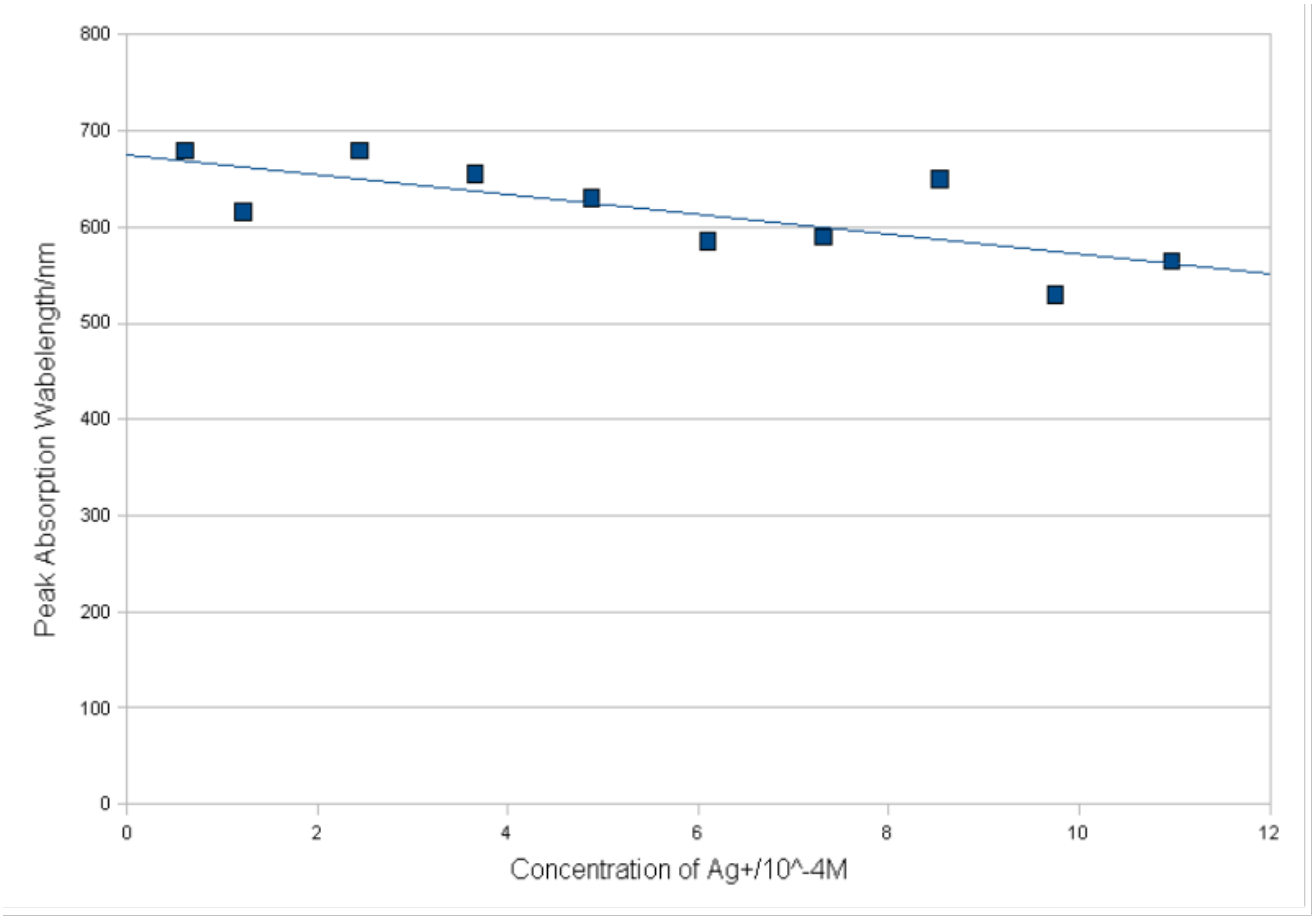

Figure 7: *The decreasing wavelength of the peak absorption of the nanoparticles produced by increasing the concentration of silver nitrate in the initial reactants. Note the convergence to the peak absorption wavelength of citrate nanospheres at 525nm*

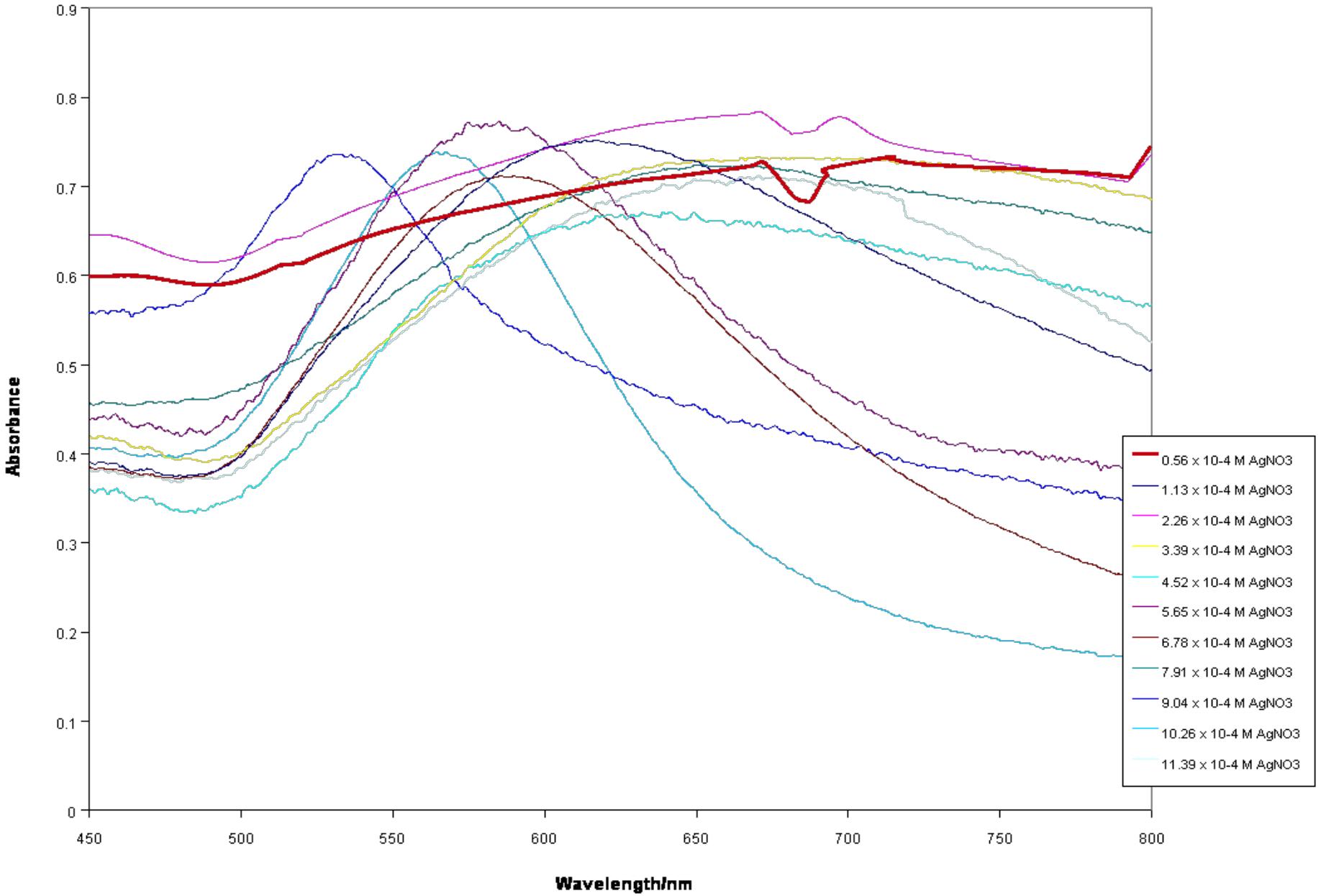

Figure 6 The UV-Vis absorption spectra of the nanoparticles produced by altering the concentration of Silver Nitrate

5.2 The Effect of Altering the Concentration of Ascorbic Acid on the Characteristics of Branched Nanoparticles

As discussed in section 3, ascorbic acid acts as a reducing agent in the reaction. This may affect many factors in the reaction, concerning the concentration Au^{+} in the solution and subsequently the rate at which the reaction occurs. There is also speculation that the ascorbic acid may act as an etching agent on the initial seeds, which may subsequently cause more nucleation sites for arm growth to be available. Thus ascorbic acid maybe an important reactant for determining the degree of branching that a nanoparticle generates. Experiments were carried out using the method described in 4.3 but with the following modifications; The concentration of ascorbic acid was changed between experiments to cover the following concentrations of ascorbic acid: 0.0788M, 0.1182M, 0.1576M, 0.2364M, 0.3152M, 0.394M, 0.4728M, 0.5516M, 0.6304M, 0.7092M ascorbic acid.

5.2.1 Modification of Physical Properties

The experiments confirm that increasing the concentration of ascorbic acid in the reaction increases the number of branches that branched particles have. Figure 8 shows a steady, if slow linear increase in the mean number of branches that are formed, with the dispersity (as measured by the standard deviation of the sample set) of the population produced remaining relatively constant for all concentrations of ascorbic acid used. However, the growth of the particles is increased in all directions, causing the core size of the particles to grow substantially as the concentration of ascorbic acid is increased. This is shown in figure 9. This core growth is insubstantial up to a concentration of 278.6×10^{-4}M, but then increases rapidly to average over 200nm in size. Particles of this size are unable to remain as a colloid when in solution with water, and as such are not useful in optical application. This is shown by the lack of spectra obtainable for these particles, as shown in figure 12. This maybe due to there not being sufficient surfactant remaining on the surface of this molecule to remain stable in colloidal solution.

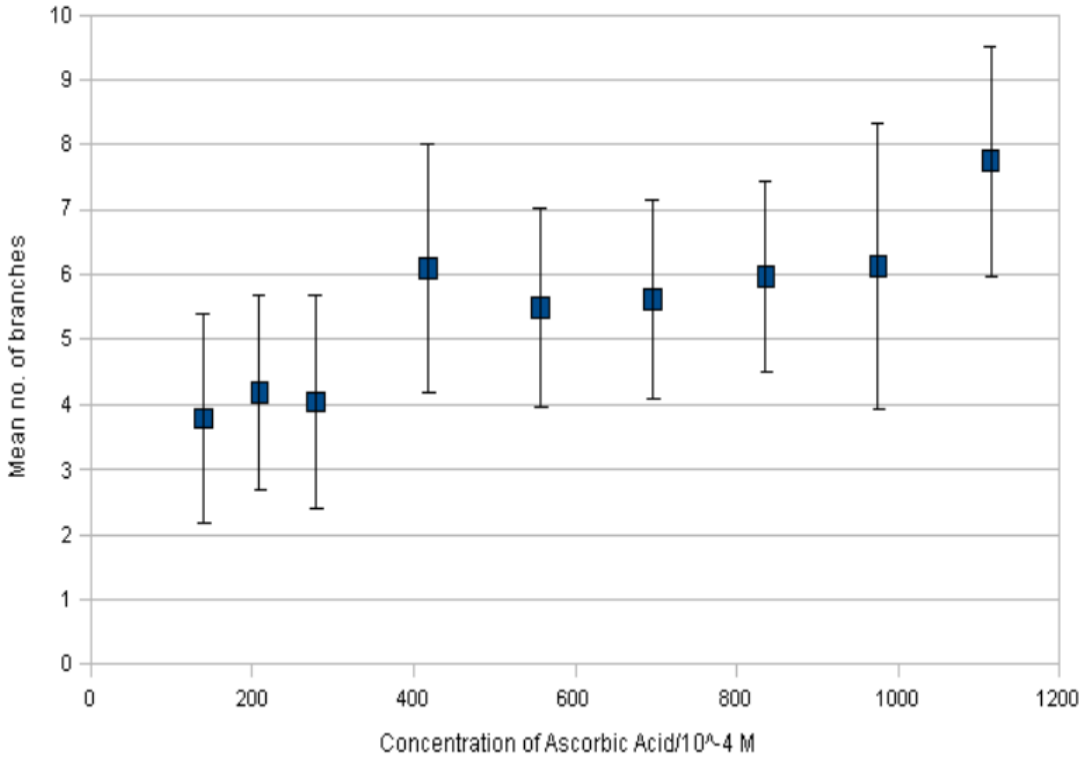

Figure 8: *The change in the mean number of branches per particle with the increase in concentration of ascorbic acid in the initial reaction.*

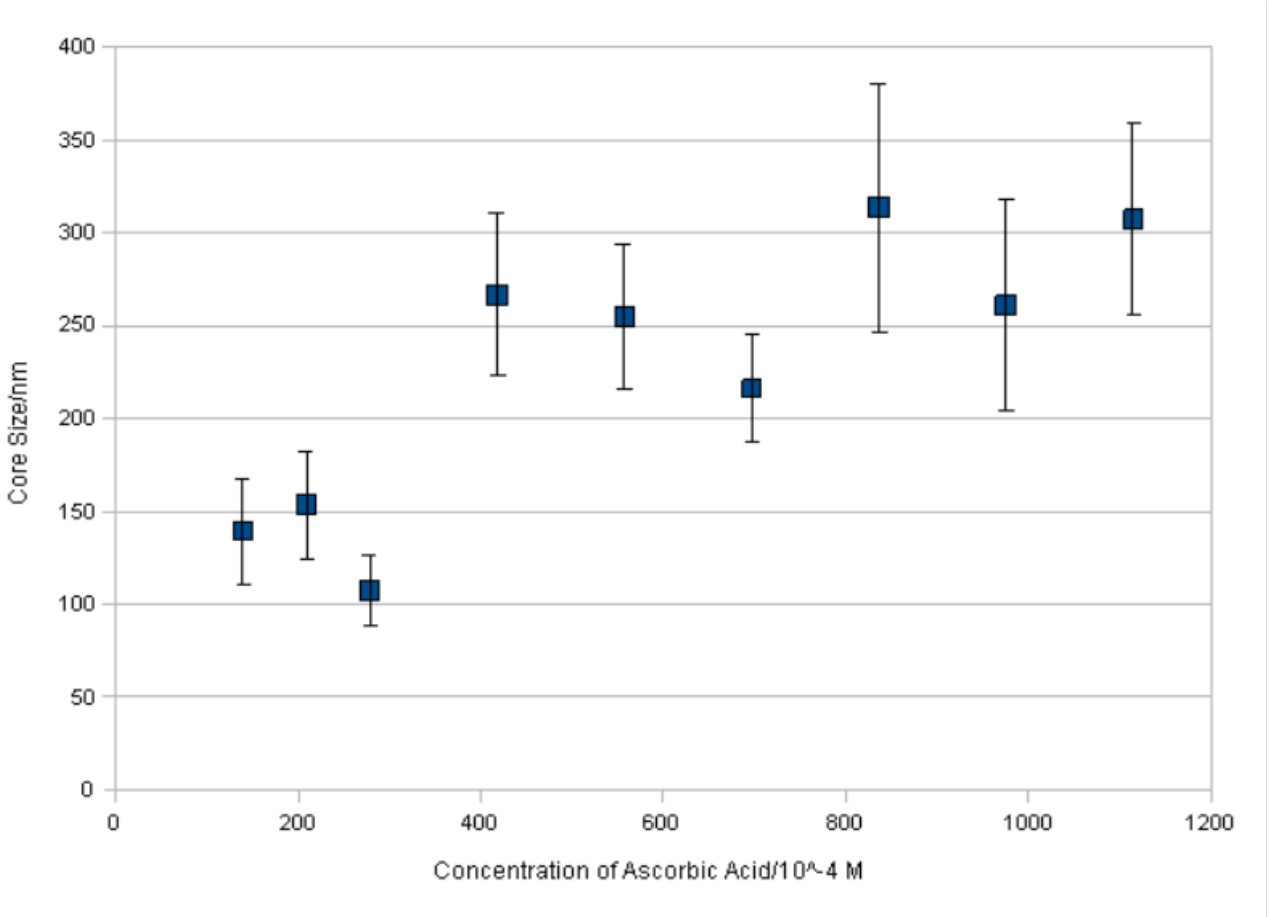

Figure 9: *The change in the core size of the particles produced due to the increase in the concentration of ascorbic acid in the initial reactants. Error bars are one standard deviation of the population of branched particles. Note the increase in this at higher concentrations indicating more disperse populations being formed*

Similarly, the length of the branches that are grown, and the width of them, increase with the increase in the concentration of ascorbic acid, illustrated in figures 10 and 11. The increase of this length is also likely to be contributing to the lack of stability as a colloid of the large core size particles. This is most likely due to a insufficient quantity of surfactant on the surface of the particle to make it stable in solution. These particles can be redispersed through the use of a sonication machine, indicating that they are not aggregations of particles.

One further result is the significant poly-dispersity of branched nanoparticles produced when a concentration of ascorbic acid greater than 278.6 x 10^{-4}M is used in the reaction method, represented by the error bars in the graphs. As can be seen in figures 9 and 10, the dispersity of the particles increases by some 50% for concentrations above that quoted above in the core size, the branch length and the branch width. This indicates that the growth of the branched nanoparticles ceases to be guided by surfactants in this regime of concentrations. This is suggestive of the monodisperse populations typically produced during surfactant guided growth.

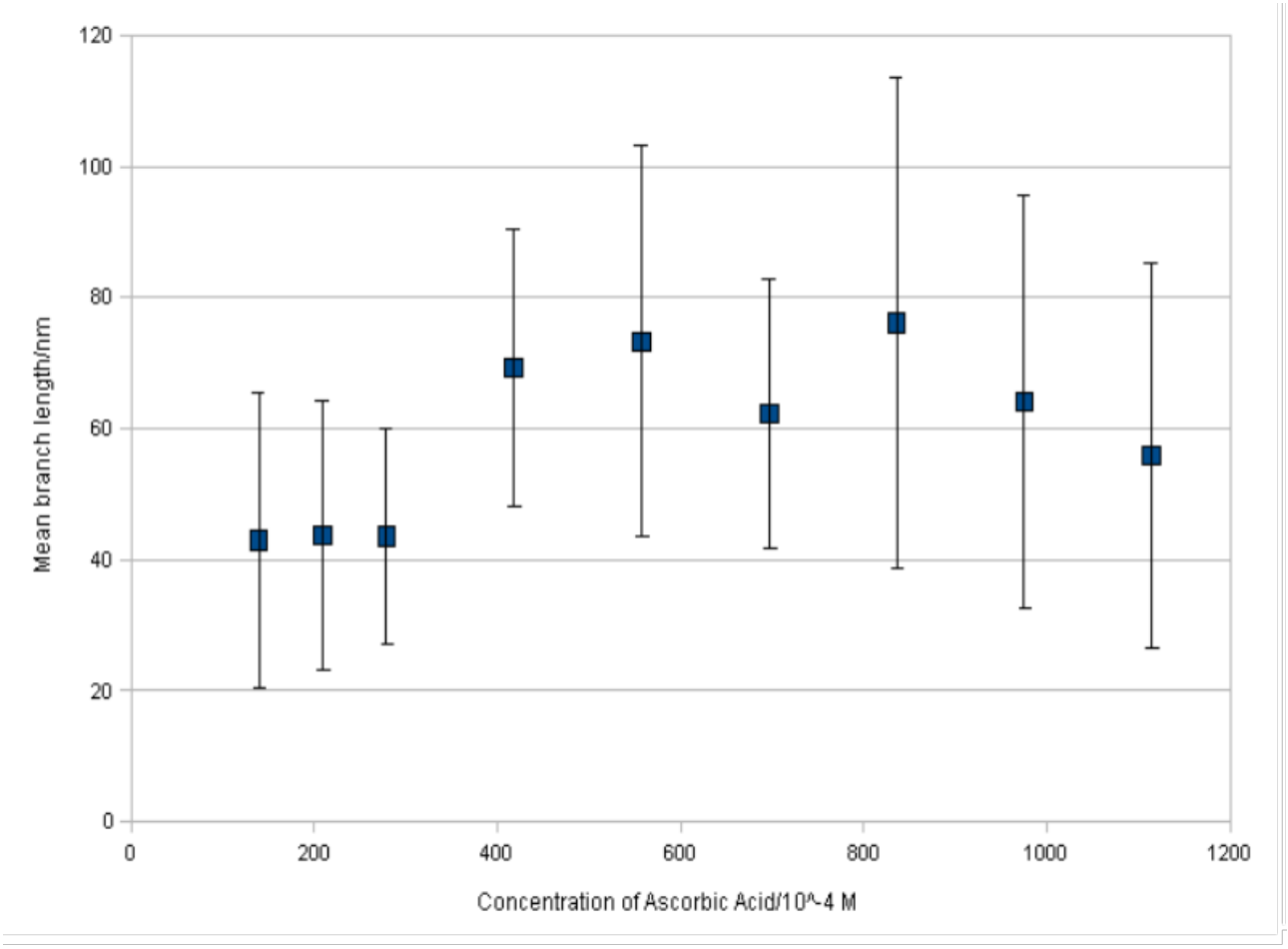

Figure 10: *The variation in the mean branch length caused by increase in the initial concentration of ascorbic acid. As with the core size, the polydispersity of the sample increases drastically above a concentration of 400 x 10^{-4}M, and the length of the branches begins to decrease as the speed of the reaction increases*

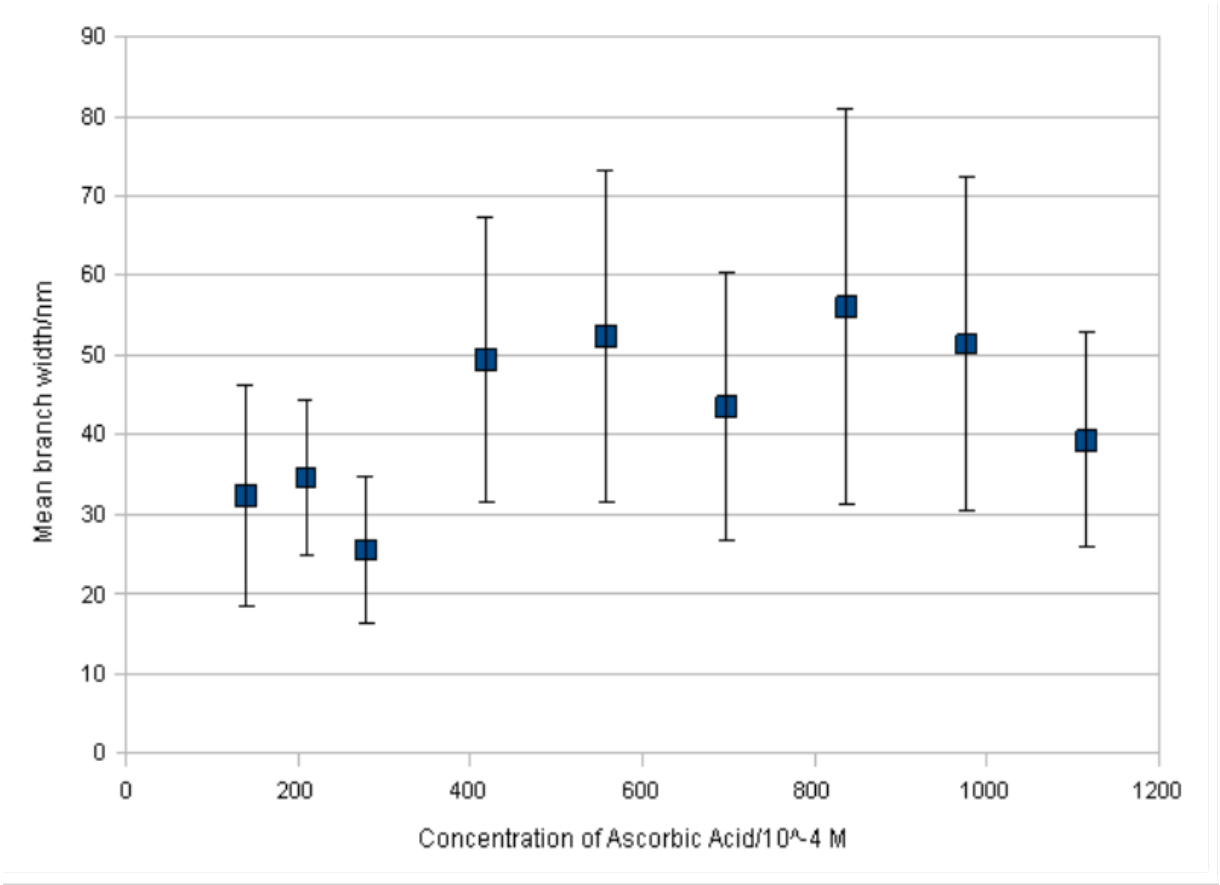

Figure 11: *The change in branch width as the initial concentration of ascorbic acid increases. The behaviour is similar to that observed in the growth of the length of the branches and the core size (figs. 9 and 10)*

5.2.2 Modification of Optical Properties

The changes in the optical properties observed from the increase in the concentration of ascorbic acid is to red shift the peak of the absorption spectra observed. This can be seen in the spectra in figure 12, where the lowest concentration of 139.3 x 10^{-4}M experiences a peak at ~560nm, is redshifted to ~650nm for colloid composed of particles made using 278.6 x 10^{-4}M and to ~800nm for a colloid made using 208.93 x 10^{-4}M. This corresponds to the increase in the mean branch length and the number of branches of the particles with the increasing concentration of ascorbic acid. This correlates with the theory in section 2.1 indicating that angular shapes on the nanoparticles act as dipoles for the SPR phenomena, as the longer arms increase the length of this dipole, and so redshift the absorption peak.

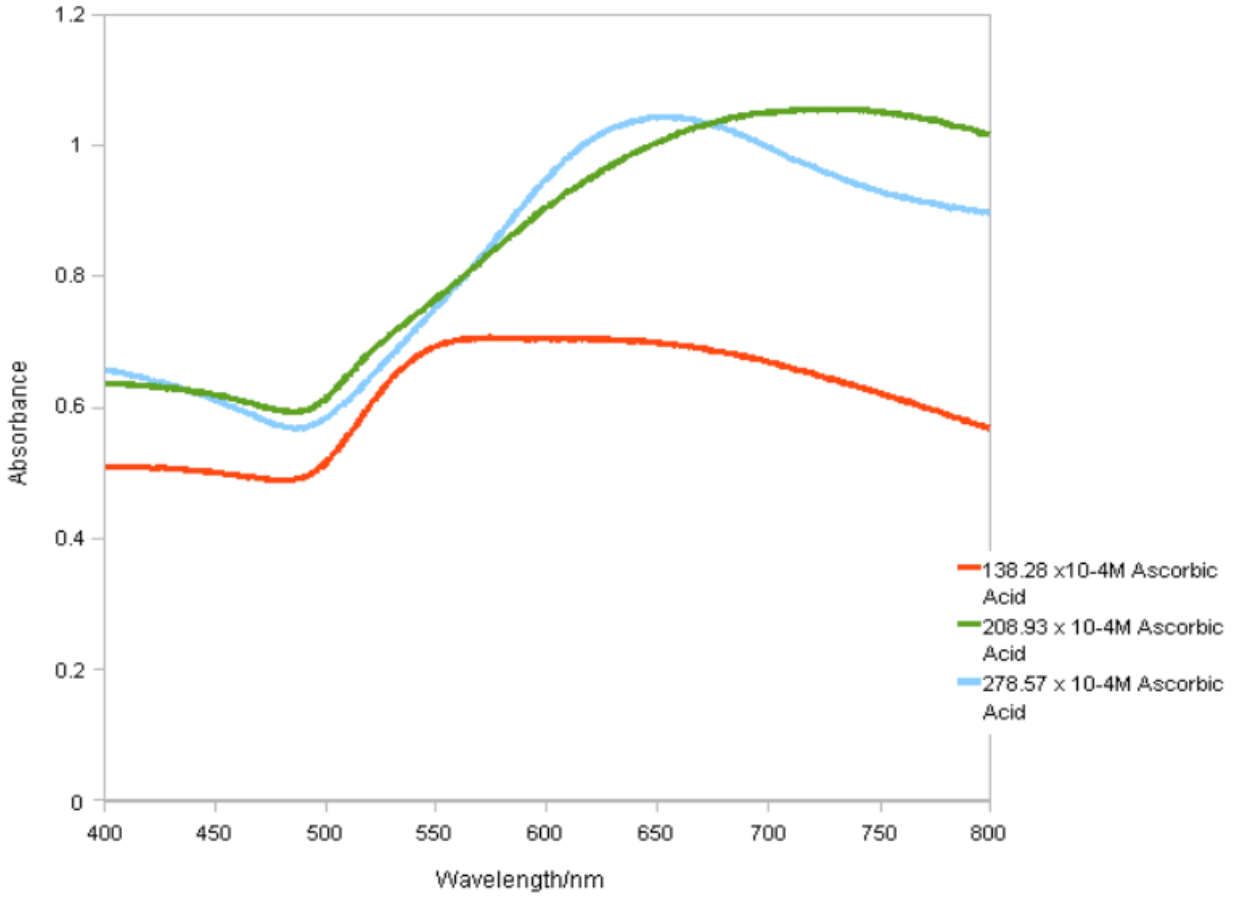

Figure 12: *The absorption spectra of the particles produced by increasing the initial concentration of ascorbic acid. Spectra for concentrations above 300 x 10^{-4}M could not be obtained as they were no longer water soluble due to a lack of surface stability.*

5.3 Modification of both parameters

The previous results had indicated that the structure of the branches produced varied when the concentrations were changed in the reaction. However, they can only be changed to a certain extent when used on their own, before unwanted side-affects (e.g. large core sizes leading the to the aggregation/insolubility of particles) occur or further development in the desired properties cannot be attained. Thus it was concluded to try and use a variety of concentrations of ascorbic acid and silver nitrate to try and combine the increased arm length and branching that ascorbic acid appears to induce, whilst controlling the reaction using silver nitrate.

The method as described in 4.3 was used, but with the following modifications to the concentration used (note - the modifications will be referred to by number from this point onwards, corresponding to their value in the list):

1. 102.5µl 10mM $AgNO_3$ and 40µl 0.1576M ascorbic acid

2. 102.5µl 2.5mM $AgNO_3$ and 40µl 0.1576M ascorbic acid

3. 102.5µl 15mM $AgNO_3$ and 40µl 0.1182M ascorbic acid

4. 102.5µl 20mM $AgNO_3$ and 40µl 0.1182M ascorbic acid

5. 102.5µl 20mM $AgNO_3$ and 40µl 0.1576M ascorbic acid

These combinations were chosen for further investigation as they combine the concentrations which have thus far produced the furthest red shifted spectral absorption peak, whilst also retaining the important property of remaining soluble in water as room temperature without large quantities of added surfactant (see sections 5.1 and 5.2).

5.3.1 Changes in Physical Properties

The changes in the physical properties observed will be compared by using samples of a constant concentration of ascorbic acid, and observing the changes caused by varying the silver nitrate. It should be noted that in all cases the dispersity will not be considered, as the dispersity of the product does not vary highly within a constant concentration of ascorbic acid.

In both series of comparisons, the size of the main body of the branched particles stayed in the region of 150-160nm, with their being a maximum in size occurring at 3.5×10^{-4}M for a constant concentration of ascorbic acid of 208.93×10^{-4}M, and minor minimum at a concentration of 2.3×10^{-4}M for a constant concentration of ascorbic acid of 278.57×10^{-4}M. However, these peaks lie within or very close to one standard deviation of the other values within their relative concentrations of ascorbic acid (shown in figures 13 and 14), possibly indicating that these are small population variations. Either way, it is confirmed that for low concentrations of ascorbic acid, the size of the core of branched nanostructures can basically be considered constant whilst the structure of the branches change.

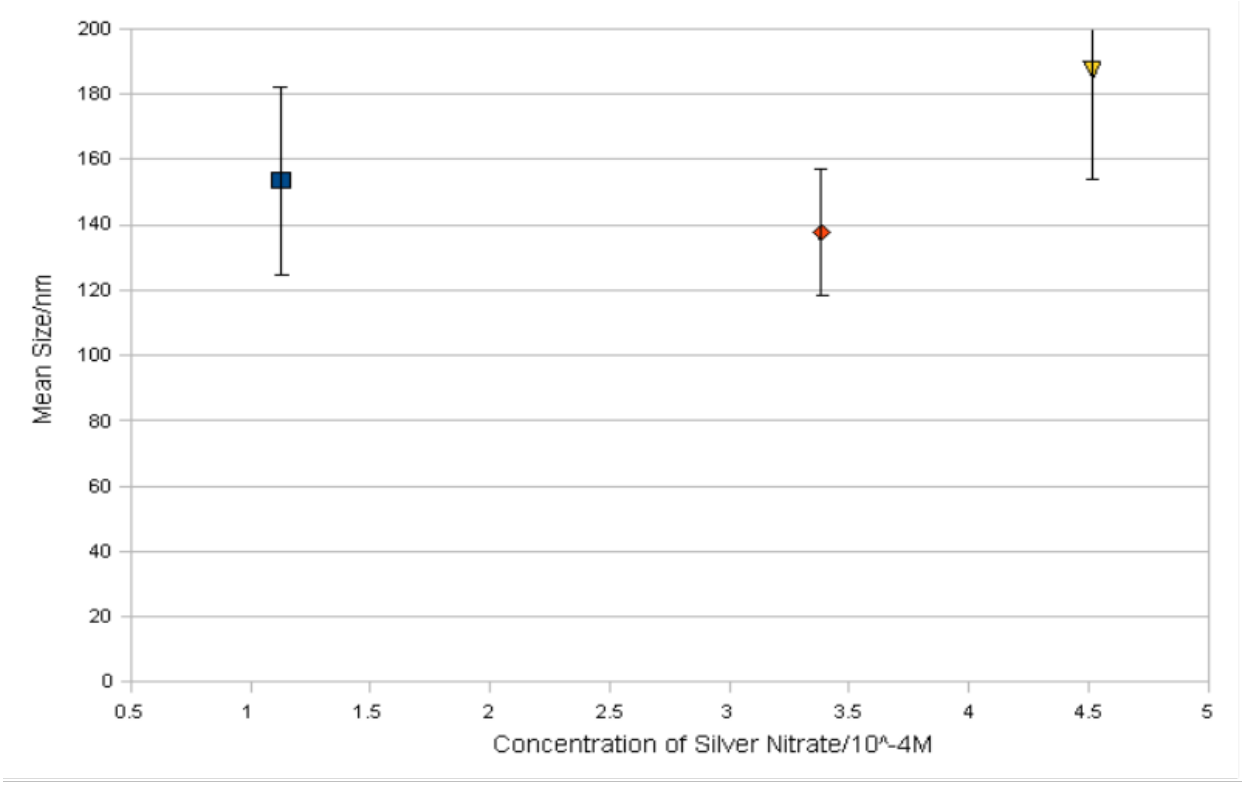

Figure 13: *The variation of the core size for changing the initial concentration of silver nitrate for a constant initial concentration of 208.93 x 10^{-4}M ascorbic acid.*

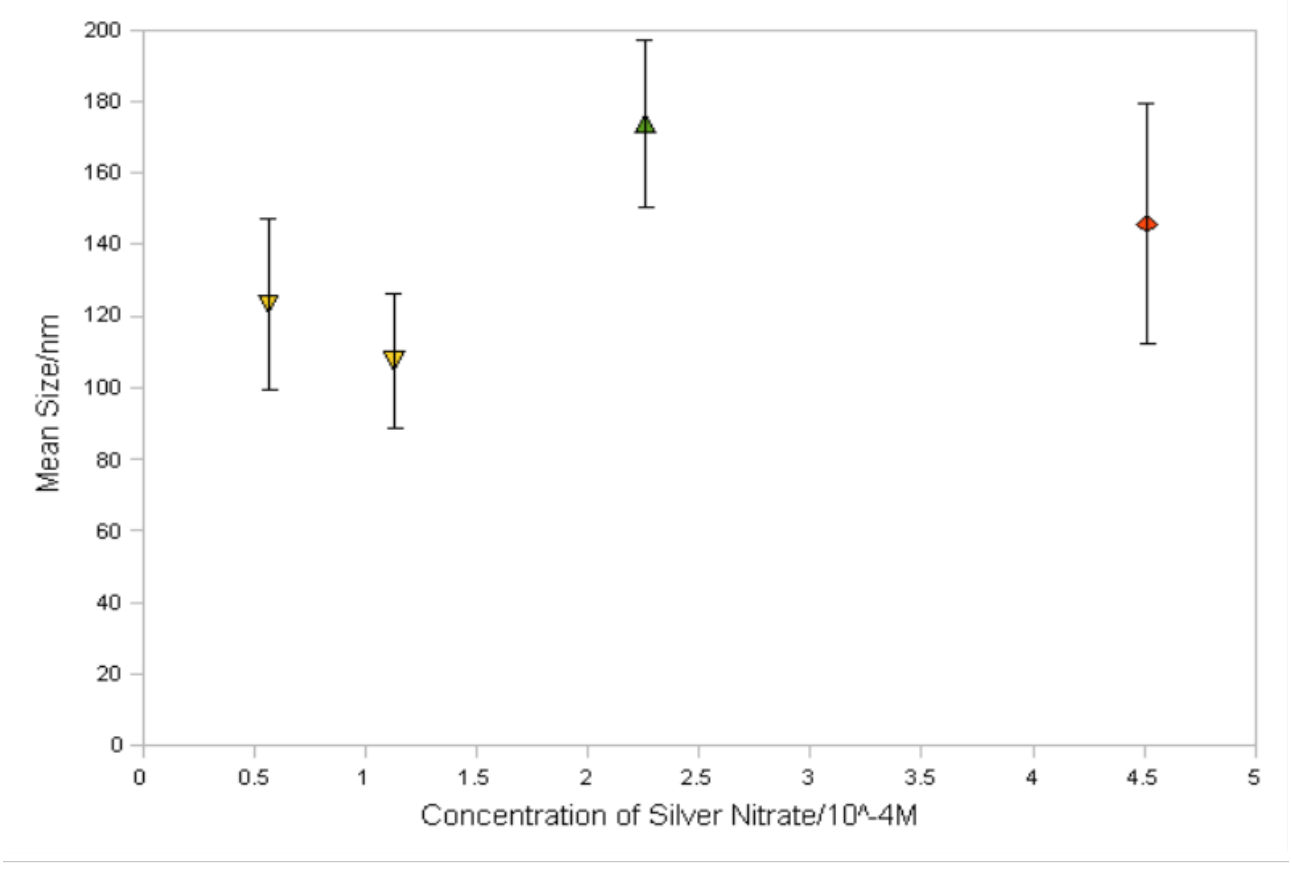

Figure 14: *The variation of the core size for changing the initial concentration of silver nitrate for a constant initial concentration of 278.57 x 10^{-4}M ascorbic acid.*

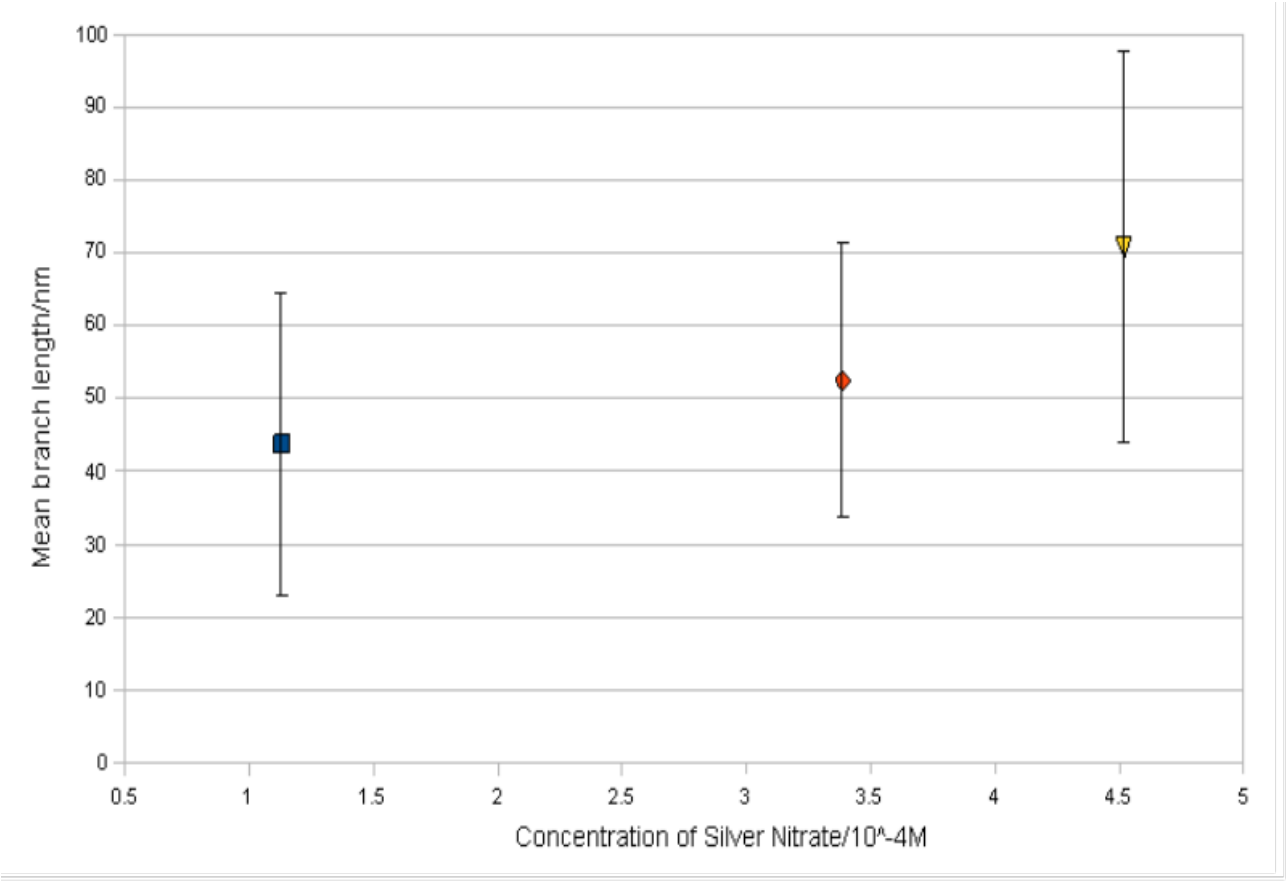

Figure 15: *The variation in the branch length produced for a constant concentration of ascorbic acid of 208.93 x 10^{-4}M.*

Considering the structure of the arms of the nanoparticles, it is shown that an increase in the mean arm length of the particles produced coincides with the concentration of silver nitrate increasing. However, the length of the arms increases significantly faster for the concentration of ascorbic acid of 208.93 x 10^{-4}M compared to the concentration of 278.57 x 10^{-4}M. They both have a similar length of 43nm at a concentration of 1.13 x 10^{-4}M silver nitrate in the solution (shown in fig 15 and 16). The concentration of 208.93 x 10^{-4}M produces a rapid growth in the final length of the arms to 52.47nm at 3.59 x 10^{-4}M and having a maximum at 70.7nm 4.51 x 10^{-4}M. Conversely, for a constant concentration of ascorbic acid of 278.57 x 10^{-4}M the growth of arms is much slower growing to 50.52nm at 2.26 x 10^{-4}M and 55.82nm at 4.51 x 10^{-4}M of silver nitrate.

The number of branches formed follows a different relationship, as it experiences in a local maximum of 6.05 branches per particle at a concentration of 3.39 x 10^{-4}M of silver nitrate for a concentration of 208.93 x 10^{-4}M of ascorbic acid and a local minimum of 4.19 branches per particle at a concentration of 1.13 x 10^{-4}M of silver nitrate and a concentration of 278.57 x 10^{-4}M ascorbic acid. The number of branches produced does not differ substantially at high concentrations of silver

for low concentrations of ascorbic acid, as is shown in fig. 17 and 18.

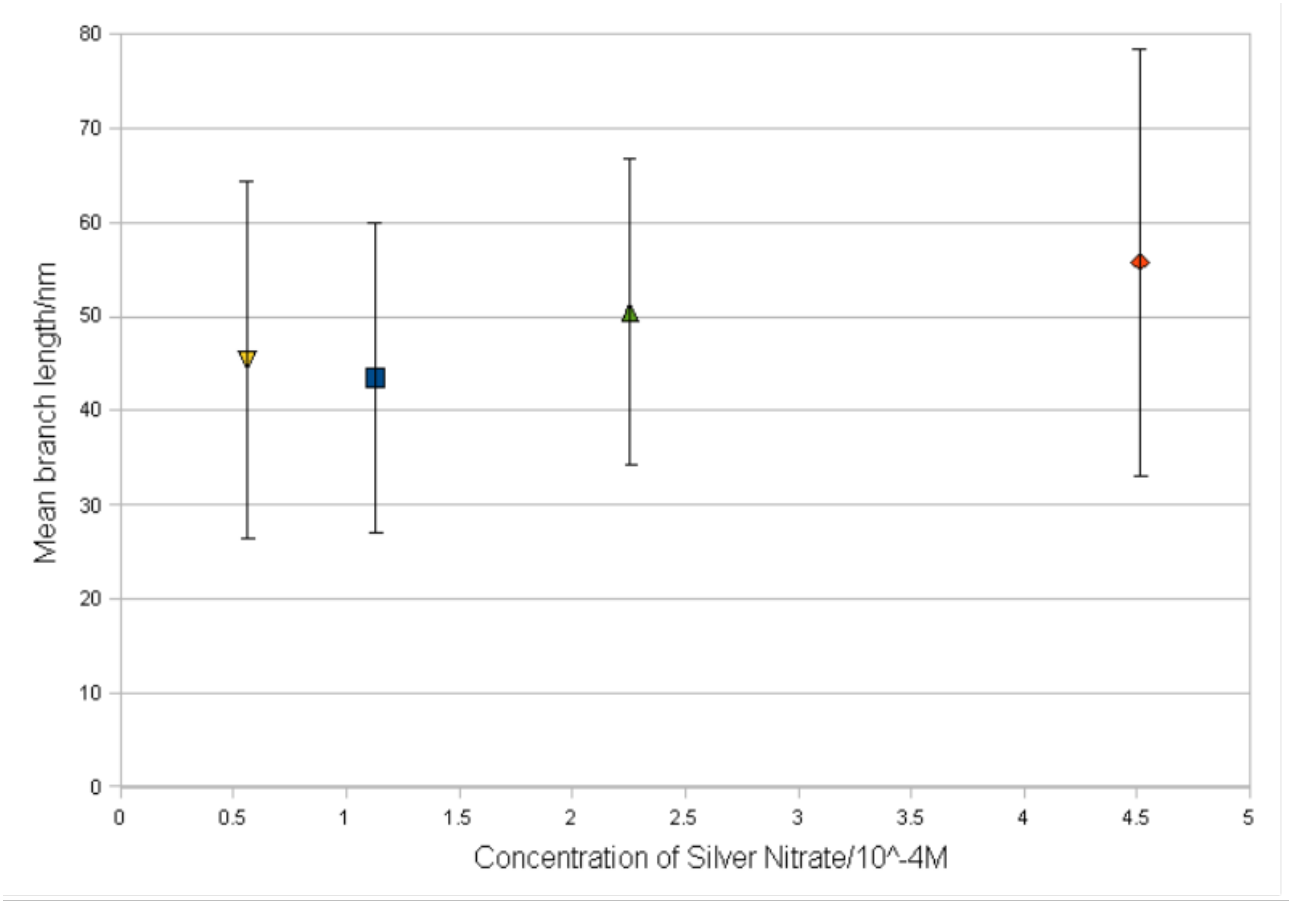

Figure 16: *The variation in the mean branch length with initial concentration of silver nitrate for a constant concentration of ascorbic acid of 278.57 x 10^{-4}M.*

It should be noted that methods (1) and (5) produced samples which were insoluble in solution with water, and methods (3) and (4) produced samples which were only soluble in low concentrations. The method (2) sample remained soluble in water. This is likely to have occurred due a lack of stabilising surfactant on their surfaces after purification. Further investigation into their solubility would be advisable.

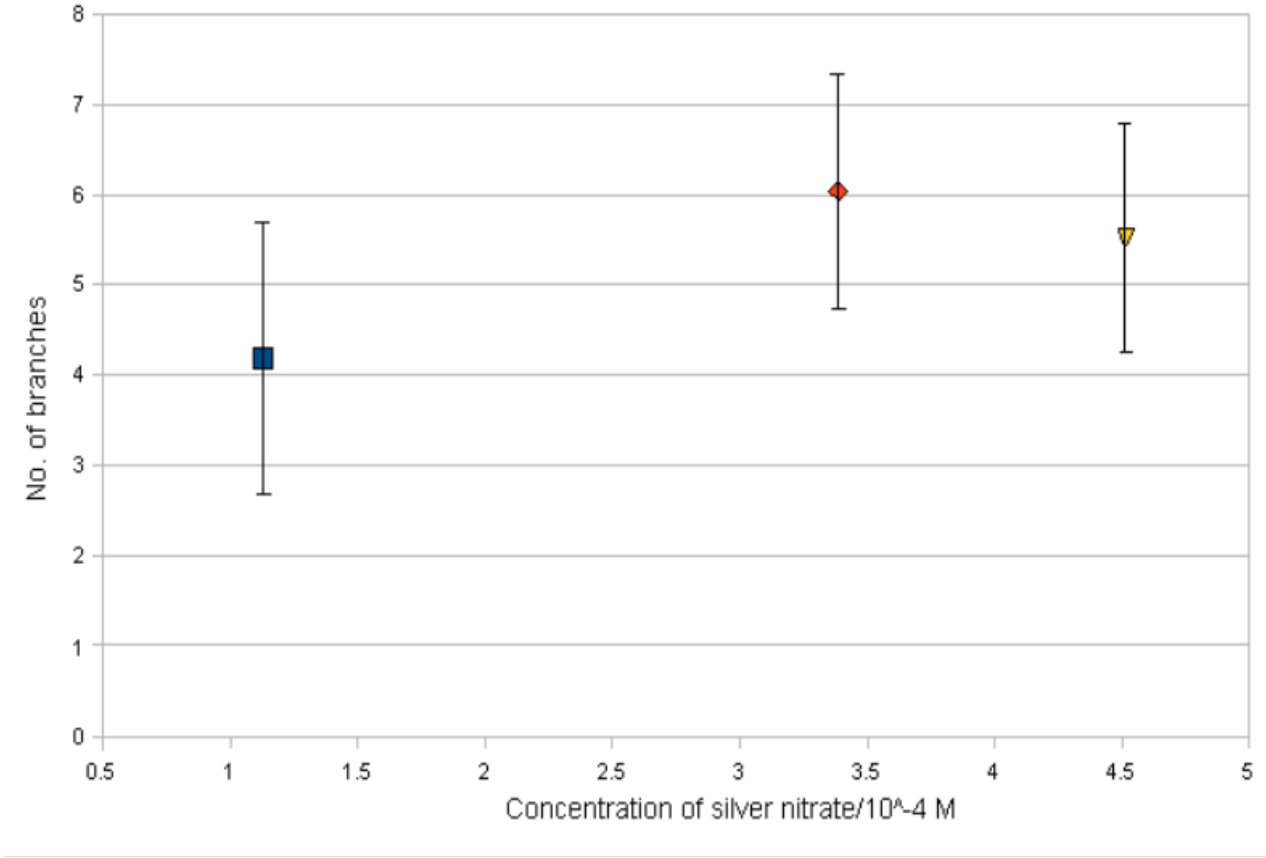

Figure 17: *The variation in the number of branches produced by varying the concentration of silver nitrate for a constant concentration of ascorbic acid of 208.93 x 10^{-4}M.*

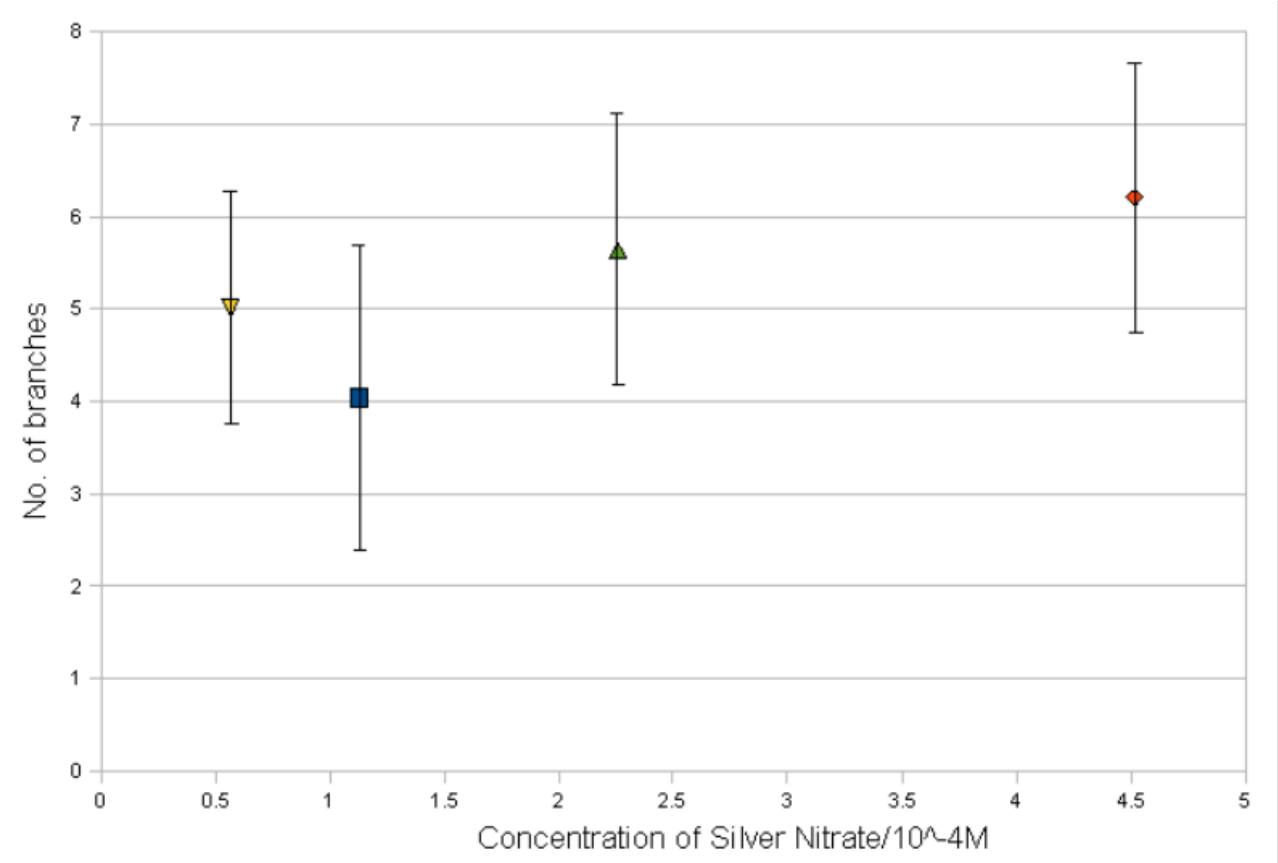

Figure 18: *The variation in the number of branches produced by varying the concentration of silver nitrate for a constant concentration of ascorbic acid of 278.57 x 10^{-4}M. Note the sharp dip at a concentration of 1.13 x 10^{-4}M. This indicates the complex relation between the reactants as this dip is not seen in fig. 16*

Figure 19: *An grid illustrating the changes in particle geometry with increasing quantities of silver nitrate and ascorbic acid. All insets are 100nm in length.*

5.3.2 Modification of optical properties

Absorption spectra could only be obtained of the method (2) sample, as it was the only sample that remained soluble at high enough concentrations to obtain a discernible spectrum. This spectrum is shown in figure 20, with the spectrum of a sample produced using the method given in 4.3 for reference. It can be seen that the peak absorption wavelength is red-shifted quite extensively, with the peak shown at ~620nm for the initial particles being redshifted to ~1µm for the method (2) sample. This falls within the “Biological NIR window", achieving one of the desired products of experiment. The peak for method (2) is also exceptionally broad, covering almost 500nm from 700nm to 1200nm at a high level of absorption/scattering. This shows promise for the use of these branched particles as a basis for SERS based bioimaging, and also for hypothermia.

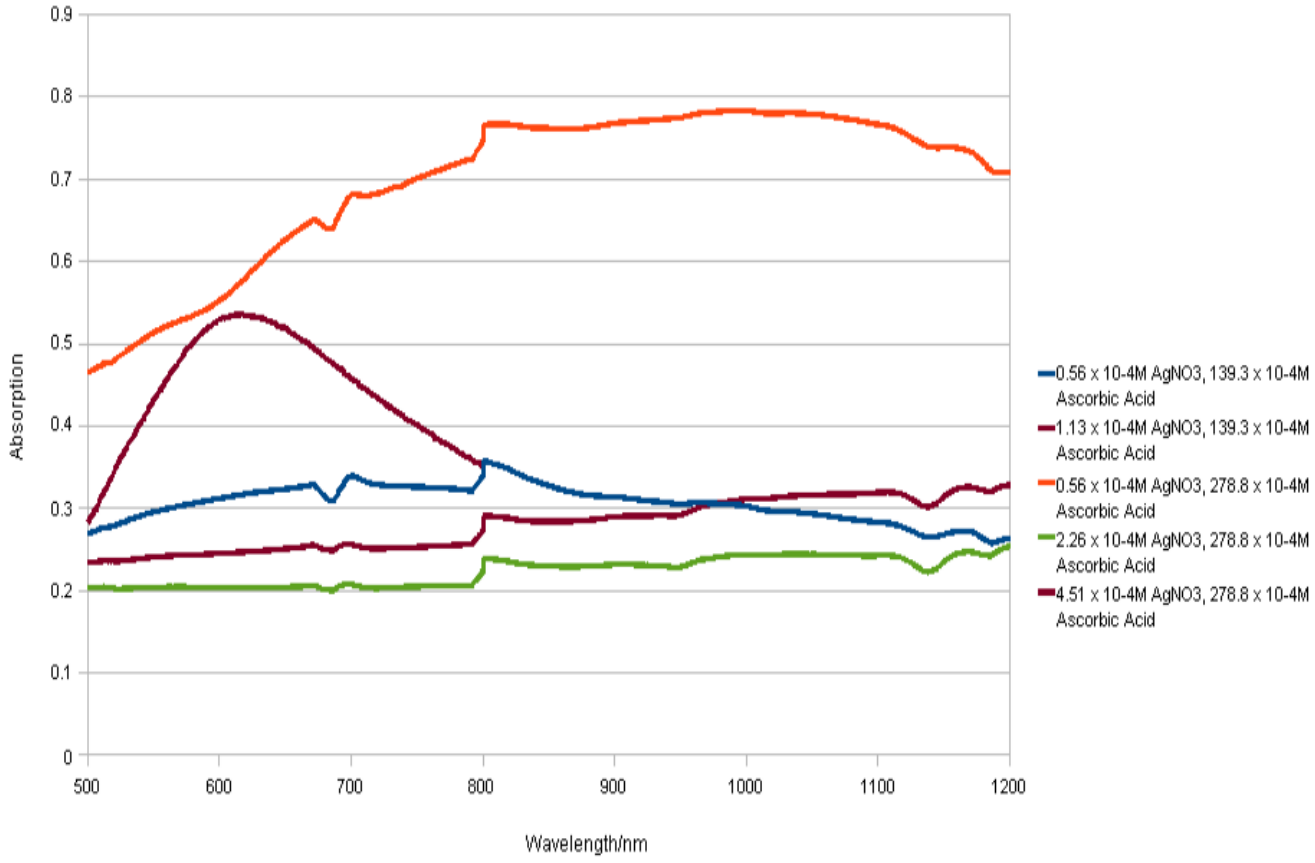

Figure 20: *The UVV absorption spectra for those samples in 1-5 that were water soluble (1,2,4,5), along with the spectra of particle produced using the method in 4.3 for comparison. Note the sudden jumps in peak are the result of bulbs changing in the UVV spectrometer. In particular not the broad absorption peak of sample 2 indicating significant scattering or many LSPR peaks across the particles.*

It is interesting to note that this large change of the absorption peak has resulted from very little change in the dimensions of the branched particles produced. The mean core size for the method (2) sample compared to the 4.3 method sample is 123nm to 139nm, mean arm length; 45nm to 43nm, mean arm width; 30nm to 32nm. The major change is the increase in the mean number of branches per particle; 5 branches per particle for method (2) to 3.8 branches per particle for 4.3 method. This correlates with the expected theory from section 2.1, as the extended profile presented by the extra branches will increase the dipole moment of the particle. This also points that if samples (3) and (5) could be made stable within solution of water by use of a higher concentration of CTAB or an alternative surfactant, they may provide even more extreme red shifting of the absorption peak due to having an average number of branches per particle above 6.

6 Conclusion

In this project it has been shown that by altering the initial reaction conditions of a wet-chemical synthesis of branched gold nanoparticles, it is possible to radically change both the physical characteristics of the particle, and also the optical properties that result from the novel structures. It has been shown that it is possible to control the core size, number of branches, length of branches and the branch width, although the dispersity of the produced samples is not completely controlled. It has also been confirmed that these changes in the structure also correspond to the red shifting of the peak absorbance wavelengths of colloidal solutions of nanoparticles. This is in good agreement with predictions from LSPR, and with previous research in the area.

We have managed to increase the peak absorption wavelength of branched nanoparticles to ~1μm whilst keeping the particles of a size such that they remain in colloidal suspension. We have also shown that the key factor in increasing the absorption wavelength seems to be a mixture of increasing the length of the branches and the number of branches themselves. This is to provide longer axes for SPR to be generated across branch and core oscillations and between branches themselves.

The results also indicate that the mechanism of the reaction used is similar to that by the Murphy group[16] to produce gold nanorods, with silver acting a preferential binding agent for surfactants to guide the growth of branches in much the same way that it encourages the anisotropic growth of nanorods, except that the larger initial seeds provide substantially more possible growth locations than do the <5nm seeds used by the Murphy method.

7 Further Research and Application

There are a number of areas that could possibly be extended into using the results of this project. Firstly, the potential of stabilising the larger nanoparticles made during this project, such as the >200nm particles shown in section 5.2.1 or those with long arms shown in section 5.3.1 should be investigated due to the interesting optical properties they may possess. Likewise, the use of these particles for optical biological application is great now that it has been shown that the peak absorption wavelength can be red-shifted far into the near-IR, and specifically the 'Biological NIR window'. This holds potential for use in hyperthermia in the treatment of cancerous diseases, and also as a non-toxic, targetable detection technique by the use of target specific ligand coating of the nanoparticles.

The use of branched nanostructures as an additive to enhance the mechanical properties of adhesives is also currently being researched, with a sample having been sent to the University of Surrey for testing on the feasibility of this idea.

Further research is also possible in determining if the use of different surfactants can further alter the controllability of the reactions, as they may offer different rates of binding thus allowing variability of the width and length of the branches. In this area also the concentration of the surfactant in the reactions has yet to be investigated, as it is unknown if the preferential binding to the Ag^+ on the surface of the seeds by CTAB is signficantly stronger than to other facets. If so, it would be possible to cause the growth of exceptionally long branch structures through reducing the concentration of CTAB.

Acknowledgements

I would like to thank Dr. Antonios Kanaras for supervising this project and giving valuable insight into the scope and details of the reactions, mechanisms and applications of the subject. I also thank Dorota Bartczak for guiding me through the initial experimental procedures and for providing continuous advice on the chemical aspects of the project and numerous hours of help in carrying out experiments and analysis. Anton Page (Biomedical Imaging Unit, Southampton General Hospital) for his assistance in utilising the TEM. Lastly I'd like to thank my lab partner Natasha Fairburn for discussion of the mechanisms of reactions, assistance in the labratory and the occassional tea break.

8 References

[1] M. Faraday, *'The Bakerian lecture: experimental relations of gold (and other metals) to light'*, Philosophical Transactions of the Royal Society of London, Vol. 147 (1847), 145-181, p. 159.

[2] Kumar, S.; Scholes, G.D.; *'Colloidal Nanocrystal Solar Cells',* Microchim Acta (2008) 160: 315–325

[3] Konjhodzic, A.; Aly, M.; Chhabria, D.; Hasan, Z.; Wu, M.; Register, R.A., '*Nano arrays of optically addressable rare earth doped semiconductor quantum dots for quantum computing'*, Proceedings of SPIE - The International Society for Optical Engineering, v 5362, p 43-51, 2004, Advanced Optical and Quantum Memories and Computing

[4] Yezhelyev, M. V.; Qi, L.; O'Regan, R. M.; Nie, S.; Gao, X., *'Proton-sponge coated quantum dots for siRNA delivery and intracellular imaging' ,* Journal of the American Chemical Society, v 130, n 28, July 16, 2008 *,* 9006-9012

[5] Choi, H.S.; Liu, W.; Misra, P.; Tanaka, E.; Zimmer, J.P.; Ipe, B.I.; Bawendi, M.G.; Frangioni, J.V., *'Renal clearance of quantum dots'*, Nature Biotechnology, Vol. 25, no. 10, OCTOBER 2007, 1165-1170

[6] Xiang, Y; Wu, Xiaochun; L, Dongfang; Li, Z; Chu, W; Feng, L; Zhang, K; Zhou, W; Xie, S; '*Gold nanorod-seeded growth of silver nanostructures: From homogeneous coating to anisotropic coating'*, Langmuir, v 24, n 7, p 3465-3470, April 1, 2008

[7] Baptista, P.; Pereira, E.; Eaton, P.; Doria, G.; Miranda, A.; Gomes, I.; Quaresma, P.; Franco, R., *'Gold nanoparticles for the development of clinical diagnosis methods'*, Analytical and Bioanalytical Chemistry, v 391, n 3, p 943-950, June 2008

[8] Dammer, O.; Vlcková, B.; Podhájecká, K.; Procházka, M.; Pfleger, J., *'Polymer composites with plasmonic metal nanoparticles'*, Macromolecular Symposia, v 268, n 1, p 91-95, July 2008, Advanced Polymer Materials for Photonics and Electronics

[9] Min, B.K.; Friend, C.M.; *'Heterogeneous Gold-Based Catalysis for Green Chemistry: Low-Temperature CO oxidation and Propene Oxidation'*, Chemical Reviews, 2007, 107 (6), 2709-2724

[10] Nehl, C.L.; Hafner, J,H, *'Shape-dependent plasmon resonances of gold nanoparticles',* Journal of Material Chemistry, 2008, **18**, 2415-2419

[11] G. Mie, “Beiträge zur Optik trüber Medien, speziell kolloidaler Metallösungen,” Leipzig, *Annual of Physics* 1908, **330**, 377–445

[12] Kelly, K.L.; Coronado, E.; Zhao, L.L.; Schatz, G.C., *'The Optical Properties of Metal Nanoparticles: The Influence of Size, Shape and Dielectric Environment'*, Journal of Physical

Chemistry B, 2003, 107, 668-677
[13] Xia, Y.; Xiong, Y; Lim, B.; Skrabalak, S.E., '*Shape-controlled synthesis of metal nanocrystals: Simple chemistry meets complex physics?'*, Angewandte Chemie - International Edition, 2009, v 48, n 1, 60-103
[14] Markov, I.V., p16, *'Crystal Growth for Beginners: Fundamentals of Nucleation, Crystal Growth and Epitaxy'*, 2nd Edition, Published Aug 2003, World Scientific Publishing Company
[15] Lu, L.; Kelong, A.; Ozaki, Y.; *'Environmentally Friendly Synthesis of Highly Monodisperse Biocompatible Gold Nanoparticles with Urchin-like Shape'*, Langmuis, 2008, 24, 1058-1063
[16] Murphy, C.J.; Sau, T.K.; Gole, A.M.; Orendorff, C.J.; Gao, J.; Gou, L; Hunyadi, S.E.; Li, T. *'Anisotropic Metal Nanoparticles: Synthesis, Assembly, and Optical Application'*, Journal of Physical Chemistry B 2005, 109, 13857-13870
[17] Kawamura, G.; Yang, Y.; Fukuda, K; Nogami, M., *'Shape control synthesis of multi-branched gold nanoparticles'*, Materials Chemistry and Physics, 115 (2009), 229-234